Available online at www.sciencedirect.com
SCIENCE DIRECT
Journal of Colloid and Interface Science 299 (2006) 530–536
JOURNAL OF Colloid and Interface Science
www.elsevier.com/locate/jcis

Adsorption of chromium ions from aqueous solution by using activated carbo-aluminosilicate material from oil shale

Reyad Awwad Shawabkeh

Department of Chemical Engineering, Mutah University, 61710 Al-Karak, Jordan

Received 15 December 2005; accepted 16 February 2006

Available online 19 April 2006

Abstract

A novel activated carbo-aluminosilicate material was prepared from oil shale by chemical activation. The chemicals used in the activation process were 95 wt% sulfuric and 5 wt% nitric acids. The produced material combines the sorption properties and the mechanical strength of both activated carbon and zeolite. An X-ray diffraction analysis shows the formation of zeolite Y, Na-X, and A-types, sodalite, sodium silicate, mullite, and cancrinite. FT-IR spectrum shows the presence of carboxylic, phenolic, and lactonic groups on the surface of this material. The zero point of charge estimated at different mass to solution ratio ranged from 7.9 to 8.3. Chromium removal by this material showed sorption capacity of 92 mg/g.

Keywords: Activated carbo-aluminosilicate; Adsorption; Sulfuric and nitric acids; FT-IR; XRD; Chromium

1. Introduction

Activated carbon and zeolite are well known materials used extensively in solid–fluid separation and chemical reactions. The microporosity and high surface area and charge for both materials highlighted them as ion exchangers, adsorbents, catalysts and separation media. Activated carbon has been widely used in chemical purification systems to remove solutes and gases from downstream. It has a specific affinity toward non-polar compounds such as organics as it has a hydrophobic property in aqueous solution.

Synthesis of activated carbon can be obtained by physical treatment, in which the surface of the carbonaceous material is exposed to a stream of gases at high temperature or chemical one where the carbonaceous material is exposed to activation agents such as acids, hydroxides and zinc chloride at low temperature (mainly less than 500 °C). The major raw materials for production of activated carbon are wood [1], coal [2], nutshells [3–5], and fruit stones [6,7]. The main disadvantage of activated carbon is the weak mechanical properties of its surface and that it is easily burned at high operation temperature [8]. On the other hand, zeolites and aluminosilicates have a good supportive material as catalysis and ion exchangers [9,10]. They have a hydrophilic affinity toward polar molecules as a result of existence of aluminum atoms in their structure. Synthesis of zeolite could be attained by treatment of aluminosilicates with alkali or alkali earth hydroxides at elevated temperature and pressure [11].

Great efforts were performed to enhance both physical and chemical properties of activated carbon and aluminosilicates materials in order to enhance their surface coverage and selectivity toward target solutes, as well as their catalytic properties. These research areas focused on synthesizing new activated carbon [12,13] and zeolites [11], impregnating their surfaces with different transition metals [14,15] or producing carbon-aluminosilicates from coal waste minerals [16].

On the other hand, chromium is one of the toxic heavy metals present in the effluents of metallurgic, galvanoplastic, textile, tanning and paint industries, which could be treated using different technological treatment methods [17–19].

In addition to the research that performed in utilizing different adsorbent for removal of pollutants from downstreams, this work focuses on synthesis of an activated carbo-aluminosilicate

E-mail address: rshawabk@mutah.edu.jo.

0021-9797/$ – see front matter
doi:10.1016/j.jcis.2006.02.058

material from oil shale and its utilization for remediation of chromium ions from aqueous solutions.

2. Experimental

2.1. Materials

Oil shale was collected from El-Lajjun area, Al-Karak County, Jordan. Sodium and potassium hydroxide pellets (>98.5% purity), potassium nitrate, concentrated sulfuric, hydrochloric, and nitric acids were supplied by Sigma Chemical Company. Atomic absorption standard of potassium dichromate (1000 mg/L) was provided by Scharlau, Spain. All solutions were prepared using deionized water from a Milli-Q system (Millipore, France). All glassware were Pyrex washed with soap, rinsed with nitric acid and washed with deionized water.

2.2. Activation

Rocks of oil shale were collected, crushed and sieved to different particle sizes and stored for further treatment. Sample of 200 g of fine particles (<45 μm) was mixed with 400 ml of concentrated sulfuric (390 ml) and nitric acid (10 ml) solutions. The mixture was then heated to 270 °C while stirred using glass rod. Meanwhile, air was sparged into the solution with flow rate of 1.0 L/min to enhance the oxidation of the mixture. Once the solution gets solidified, it was removed out of the hot plate and allowed to cool down at room temperature, then washed with deionized water to remove any adhered acids. Then the activated material was mixed overnight with 100 ml of 1.0 M sodium hydroxide. After that, the mixture was heated in a closed vessel in oven at 160 °C for 8 h. The resulting material was washed with deionized water, dried at 105 °C and stored in closed containers for further uses.

2.3. Characterization

Physical and chemical characteristics of oil shale were estimated by measuring the total volatile and organic matters, moisture and ash content, and total sulfur and carbonates. A sample of oil shale was introduced into a glass vial and heated at 70 °C for 30 min [20]. The volatile gas was collected and analyzed using Shimadzu GC-MS spectrophotometer. Moisture content was then determined using xylene-extraction test method (ASTM D 2867-95). Accurate weight of 25 g of oil shale was put into a boiling flask and a 100 ml of xylene was added. The flask was connected to a water trap and placed onto controlled temperature hot plate to allow steady reflux of the xylene. The xylene was continued refluxing until no further water could be collected in the trap. The moisture content is calculated according to

$$\text{Moisture content} = \frac{\text{volume of collected water}}{\text{initial weight} - \text{final weight of the ash sample}}.$$

The sample that tested according to its moisture content was weighed and placed in a Muffle furnace at 950 °C for 3 h. Then it was cooled to ambient temperature in a desiccator and then weighed for its ash content. The difference in weight between the original and final sample represent the volatile matter removed during heating.

Total sulfur was determined using the modified ASTM D2392 and ASTM D3177 procedures proposed by Tuttle et al. [21]. Sample of 5 g of oil shale was mixed with 80 ml of 6 M de-areated HCl and the reaction was allowed to proceed for 15 min. During the reaction the evolved H_2S was trapped in a solution of 0.1 M $AgNO_3$ to produce Ag_2S. The remaining solution was filtered and the filtrate was treated with magnesium oxide and sodium carbonate solution (60 wt% MgO, 40 wt% Na_2CO_3) and fused in a Muffle furnace at 800 °C for 2 h. The produced cake was dissolved in diluted HCl (pH 4) and mixed with 10% $BaCl_2$ and allowed to boil for 15 min. The precipitated barium sulfate represents the acid soluble sulfate in the sample. The disulfide compounds were determined by treating the remaining residue of the sample with 50 ml (1 M) chromium(II) and 20 ml HCl solution. The evolved H_2S was again trapped as in the above procedure and the weight of Ag_2S was recorded. Similar procedure to the acid soluble sulfate was performed on the remaining residue for determination of total bound organic sulfur compounds.

Total inorganic carbon was analyzed by acidification of 1 g of dry oil shale sample with 50 ml of 3 N HCl solution. The mixture was boiled for 5 min, cooled, filtered and all the remaining acid in the sample washed with water. The amount of unused acid was determined by back titration with 0.25 N sodium hydroxide using phenolphthalein as an indicator [22]. Then the amount of carbonate was measured according to

$$\text{Amount of carbonate} = \frac{5\ (\text{meq. HCl added} - \text{meq. NaOH used})}{\text{weight of the sample}}.$$

This method usually provides the percentage of carbonate with an error of ±5% due to reaction of other alkali carbonates with acid, which are considered negligible with respect to calcium carbonate.

Fourier transform infrared spectrophotometry (FT-IR) analysis was conducted for the produced samples by mixing a pre-dried sample of 3.0 mg with blank KBr and pressed hydraulically at 10 tons/m^2 to obtain a thin transparent disk, then analyzed using 8400S Shimadzu spectrophotometer. Imaging microscope analysis was performed using an Olympus MIC-D digital microscope.

X-ray diffraction spectroscopy (XRD) analysis was carried out with PANalytical X-ray, Philips Analytical. A dried sample of the produced material was ground using an agate mortar and pestle and tested at 40 kV and 40 mA.

The pH_{ZPC} for the produced material was determined by introducing 0.5 g of carbo-aluminosilicate into six 100-ml Erlenmeyer flasks containing 50 ml of 0.1 M potassium nitrate solution. Initial pH values of the six solutions were adjusted to 2, 4, 6, 8, 10, and 12 by either adding few drops of nitric

acid or potassium hydroxide. The solution mixtures were allowed to equilibrate in an isothermal shaker (22 ± 1 °C) for 24 h. Then the suspension in each sample was filtered and the final pH was measured again. The procedure was repeated by varying the mass of carbo-aluminosilicate introduced into the solution from 0.05 to 0.5 g.

2.4. Chromium isotherm

Adsorption tests were conducted in 100-ml Erlenmeyer flasks. A sample of 0.1 g of carbo-aluminosilicate material (particle size <45 μm) was mixed in 50 ml solution of different potassium dichromate concentrations (25–300 mg/L) and allowed to equilibrate in the isothermal shaker (22 ± 1 °C) for 24 h. The pH was adjusted to 4 by addition of a few drops of either hydrochloric acid or potassium hydroxide. Similar procedure was performed in order to obtain the adsorption isotherm at pH 7.5. Blank solutions containing either potassium dichromate or carbo-aluminosilicate where also put in the shaker and treated similarly to the above procedure. After 24 h, all solutions were filtered and centrifuged to remove any suspensions and then analyzed using S4 ThermoElemental atomic absorption spectrophotometer. The difference between the initial and final concentration of each ion represents the amount that transferred to the surface of the carbo-aluminosilicate.

3. Results and discussion

The chemical analysis of El-Lajjun oil shale is presented in Table 1. The studied samples provided 25.9 wt% of organic and volatile matter while 54.5 wt% of ash. The composition of the ash showed 27.5 wt% silica and 4.8% alumina while the rest are alkali and alkali earth oxides.

The oil shale samples were treated with both sulfuric and nitric acids. The activation was performed by addition the sulfuric acid to the shale samples at room temperature where no effect was noticed on the mixture. Then the nitric acid was added gradually to the mixture, which resulted in a rapid increase in the solution temperature to 150 °C, reached within 1 min as a result of exothermic reaction. Then the solution was heated further while carbon monoxide, carbon and sulfur dioxide, and nitrous oxide were released out of the solution [23]. Upon activation with these acids, several sulfonation and nitrification reactions took place at the surface of the oil shale samples yielding an activated carbon with surface functional groups according to Scheme 1 [24,25].

Table 1
Chemical analysis of El-Lajjun oil shale

Property	Value (wt%)
Organic matter	22
Volatile matter	3.9
Ash	54.5
Moisture	3.1
Sulfur	2.6
Carbonates	13.9

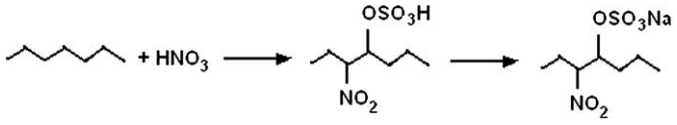

Scheme 1. Sulfonation and nitrification reactions at the surface of carbo-aluminosilicate.

Also, treatment with the acids changed the composition of the ash in the sample where a chemical reaction took place between the calcium ions in the lime and the sulfate and nitrate in the acidic solution leading to the formation of calcium sulfate and nitrate. This could be leached out of the solid matrix during washing through leaving a structure of alumina and silica. Further treatment of this alumina and silica-based solid material with sodium hydroxide allows further reaction on the surface of the produced activate carbon and cross-linked silica and alumina structures to form zeolite materials.

A FT-IR spectroscopic study for the activated solid materials shows different functional groups as illustrated in Fig. 1. It is clear three major absorption bands at 3300–3600, 1400–1700, and 1050–1200 cm^{-1}. The spectra showed a wide band with two maximum peaks at 3420 and 3566 cm^{-1}. This band can be assigned to the O–H stretching mode of hydroxyl groups and adsorbed water. Moreover, this broad peak band in the range of 3200–3650 cm^{-1} is attributed to the hydrogen-bonded OH group of alcohols and phenols [26,27]. In the 1050–1200 cm^{-1} regions, peaks at 1093 and 1101 cm^{-1} might be related to the carbon–oxygen dingle bonds displayed stretching in acids, phenols, ethers, and esters [27]. In the region 500–900 cm^{-1}, there is a peak at 603 cm^{-1} which is assigned to C–H out-of-plane bending in benzene derivative. The peak at 1456 cm^{-1} appeared due to C=C stretch in aromatic rings [28]. The peaks at 1600–1700 cm^{-1} are due to the double bond C=O stretching vibrations with aromatic carbons [29,30]. The absorption peak near 1699 cm^{-1} is attributed to carboxylic group appeared as oxidation by nitric acid followed by hydroxide treatment [31]. The band at 2343 cm^{-1} is ascribed to the carbon–carbon triple bond vibrations in alkyne group [26]. The shoulders observed at this band are usually ascribed to the presence of aliphatic compounds [32].

X-ray diffractogram for the produced carbo-aluminosilicate is shown in Fig. 2a. The XRD spectra illustrated the presence of mullite, sodalite, quartz, and zeolite. Quartz appeared at 21° 2θ, hydroxyl-sodalite at 24° 2θ, zeolite A at 27° 2θ, zeolite Na-X at 31° 2θ. Other peaks where located at 36° and 45° 2θ for zeolite A, while the rest of the peaks are for mullite, cancrinite, sodalite, or sodium silicates. On the other hand, XRD for oil shale shows major peaks of feldspar, quartz, calcite, and anhydride at different 2θ values, as shown in Fig. 2b.

Fig. 3 shows the imaging microscope photographs for the produced material. It is clear that irregular and porous surface may be observed where the dark area represents the carbonaceous materials surrounded by the aluminosilicates (a white one).

The zero-point of charge for the activated sample was taken into consideration before determining its removal capacity

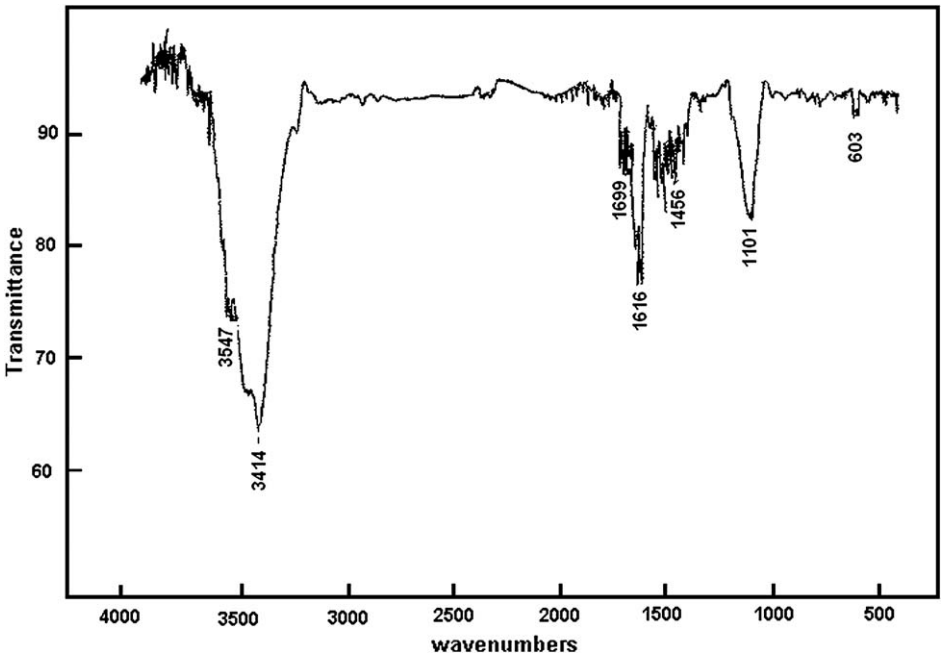

Fig. 1. FT-IR spectrum of activated carbo-aluminosilicate material.

against the metal of interest. This ZPC determines the electrophoretic mobility where the net total particle charge is zero. The produced material is composed of three main constituents, silica which has a $pH_{ZPC} = 1.9$, alumina ($pH_{ZPC} = 9.5$), and activated carbon ($pH_{ZPC} = 5$–8) [33]. Combining these three constituents resulted in strong attraction of their surfaces due to electrostatic attraction of the opposite sign of these surfaces yielding a pH_{ZPC} value in the range of 7.9–8.3, as shown in Fig. 4a. It is evident that this surface exhibits amphoteric properties, and acts as a buffer in a wide pH range of 3 to 9 were the pH_{final} remains almost close to the pH_{ZPC} for all values of $pH_{initial}$ in this range. Fig. 4b shows the variation of pH_{ZPC} with the concentration of carbo-aluminosilicate in solution. An increase in solid-to-solution ratio from 1:1000 to 1:150 leads to an increase in pH_{ZPC} from 7.9 to 8.3. This is due to the dissolution and hydrolytic reactions occurring at the solid/solution interface of the carbo-aluminosilicate. The latter has an incongruent solubility as a result of different solid phases in its structure, which yields a pH_{ZPC} dependence on the solid-to-solution ratio (surface area) [34].

Chromium adsorption is shown in Fig. 5. It is clear that Cr^{6+} was strongly adsorbed at low pH and declined sharply at higher value. The variation of adsorption of chromium ions can be explained by taking into account the isoelectric point of the carbo-aluminosilicate surface and the existing forms of chromium species at different pH values.

In an aqueous solution Cr^{6+} exists in the form $HCrO_4^-$, CrO_4^{2-}, or $Cr_2O_7^{2-}$ depending on pH value, while Cr^{3+} is in the form $Cr(OH)^{2+}$ or CrO_2^- [35,36]. Upon hydration the solid surface develops hydroxyl groups which behave as Bronsted acids according to [37,38]

$$CS\text{–}OH_2^+ \Leftrightarrow SC\text{–}(OH)^0 + H^+,$$

$$SC\text{–}(OH)^0 \Leftrightarrow SC\text{–}O^- + H^+,$$

where $CS\text{–}OH_2^+$ represents the protonated surface hydroxyl groups when the solution acidity is bellow the pH_{ZPC}, $SC\text{–}(OH)^0$ illustrates the neutral surface at the pH_{ZPC}, while $SC\text{–}O^-$ is the ionized surface above the pH_{ZPC}. As the solution pH increases or decreases the speciation of the protonated or ionized surface will be increased as a result of increasing the surface charges of the functional groups. This illustrates the increase in adsorption capacity of Cr^{6+} with decreasing the solution pH. At pH 2–6, the surface of the carbo-aluminosilicate material is electropositive and attracts most chromium species that exist in solution in the form $HCrO_4^-$ while at higher pH vales the surface becomes electronegative and repulse the CrO_4^{2-} species which become predominate in solution. Therefore, the amount of Cr^{6+} uptake by the surface will be higher at pH 4 than that at pH 7. On the other hand, at highly acidic solution ($pH < 2$), the hexavalent chromium species gets reduced to trivalent ones according to

$$Cr_2O_7^{2-} + 14H^+ + 6e^- \rightarrow 2Cr^{3+} + 7H_2O.$$

Aggarwal et al. stated that the maximum adsorption of Cr^{6+} takes place at pH 3 while the maximum reduction of Cr^{6+} to Cr^{3+}, at pH 1 [39]. Similar finding was attained by Bishnoi et al. when Cr^{6+} was strongly adsorbed onto the surface of activated rice husk and alumina. The maximum chromium removal was 91% obtained at pH 4 by the surface of alumina and 80% at pH 2 by the surface of activated rice husk. Therefore, it is expected that at pH 4 only adsorption phenomena take place at the surface of the activated carbo-aluminosilicate but not reduction reaction.

The isotherm data was fitted using Langmuir and Freundlich models. Mathematical expression for the Langmuir model in terms of chromium concentration in solution, C_e (mg/L) in equilibrium with that on the solid surface, q_e (mg/g) is given

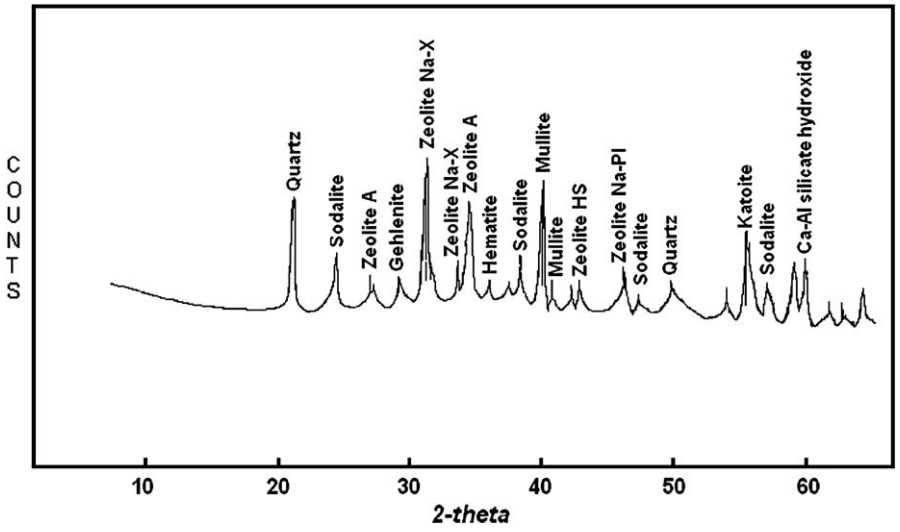

(a)

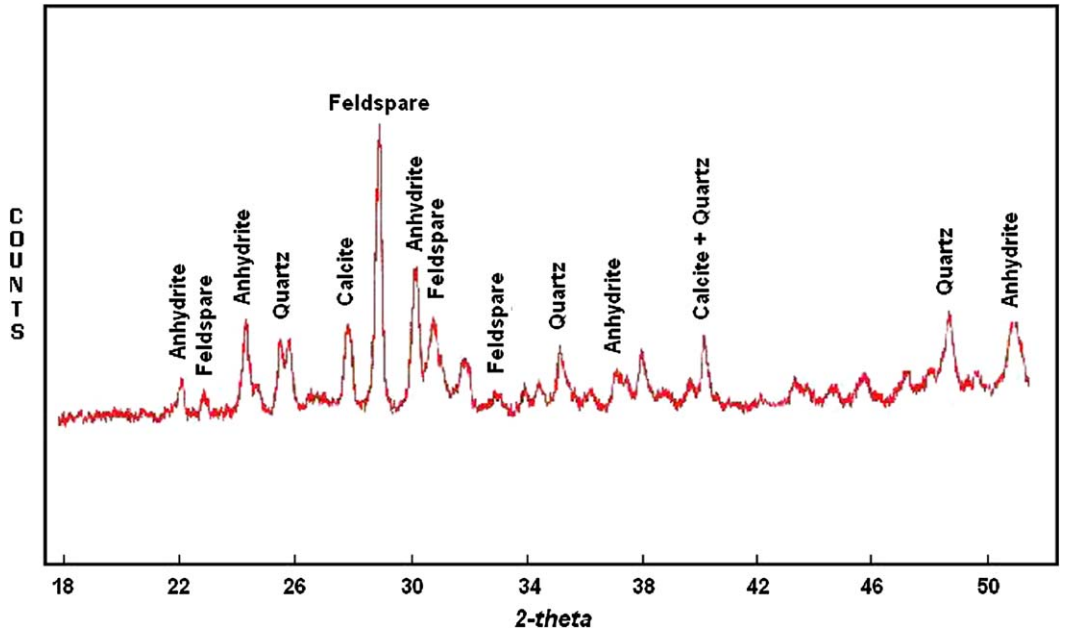

(b)

Fig. 2. X-ray diffraction patterns for activated carbo-aluminosilicate (a) and oil shale (b).

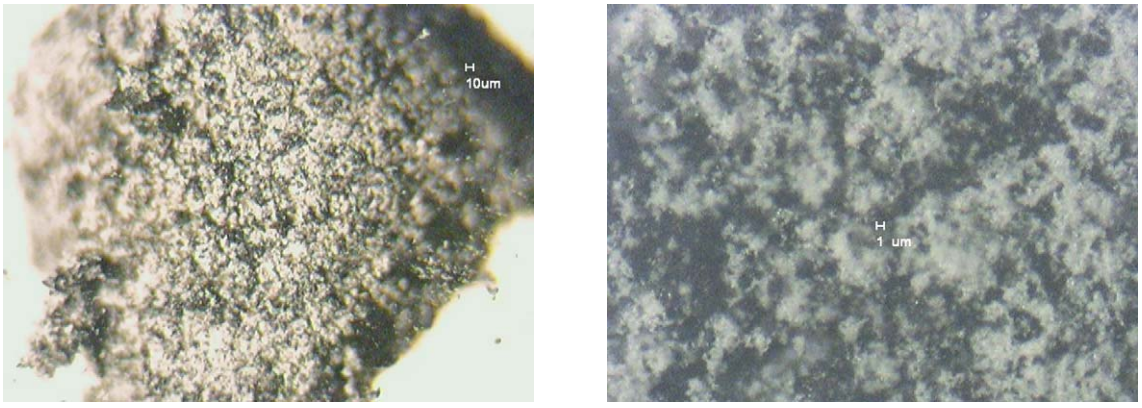

(a) (b)

Fig. 3. Imaging microscope photographs of the activated carbo-aluminosilicate. (a) 0.7×; (b) 9×.

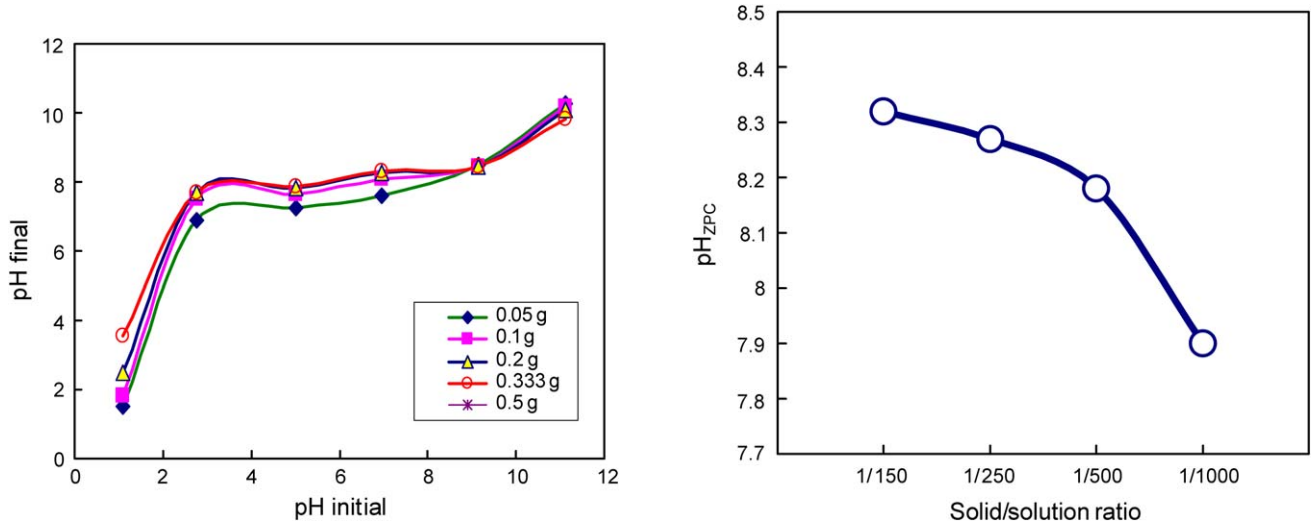

Fig. 4. (a) Variation of ΔpH_{ZPC} vs $pH_{initial}$ for the activated carbo-aluminosilicate material; (b) effect of solid to solution ratio on the variation of pH_{ZPC}.

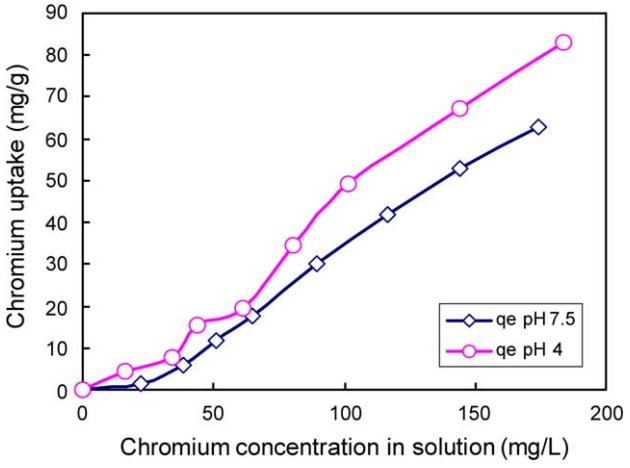

Fig. 5. Adsorption isotherms of chromium using carbo-aluminosilicate material.

by

$$q_e = \frac{QbC_e}{1 + bC_e}, \tag{1}$$

where Q (mg/g) is the maximum amount of chromium per unit mass of activated carbo-aluminosilicate required to form a complete monolayer and b (L/mg) is the Langmuir constant related to the affinity of binding sites.

On the other hand, the Freundlich equation takes the form

$$q_e = K_F C_e^{\beta}, \tag{2}$$

where K_F and β are constants. The experimental data were fitted to these models using SPSS software (version 10) and the values of both models parameters are shown in Table 2. It is clear that Freundlich model fits best the chromium isotherm at pH 4 and 7.5 with correlation coefficients of 0.995 and 0.989 and sum of square errors 33 and 48, respectively. While the Langmuir model showed a linear relation between the concentration of chromium in solution and on solid with correlation coefficients 0.910 and 0.961, and sum of square errors 607 and 167, respectively.

Table 2
Adsorption isotherm model parameter at different pH values

pH	Langmuir model	Freundlich model
4	$Q = 3.639 \times 10^5$ $b = 1.441 \times 10^{-6}$ $R^2 = 0.910$	$K_F = 0.0197$ $\beta = 1.705$ $R^2 = 0.995$
7.5	$Q = 1.734 \times 10^5$ $b = 1.993 \times 10^{-6}$ $R^2 = 0.961$	$K_F = 0.0810$ $\beta = 1.297$ $R^2 = 0.989$

4. Conclusion

Synthesis and production of activated material from oil shale that contains carbon and zeolite can be performed with low cost of raw material and safe operation. This material proved to be a good adsorbent as it has an amphoteric and hydrophilic properties in a wide range of solution acidity. It can be used efficiently for removal of chromium ions from aqueous solutions. The removal capacity was 92 mg/g. Also this material can also be utilized in heterogeneous chemical reactions as a supporting catalyst. It can tolerate compression and high temperature. Further tests on its catalytic property are recommended for future work.

References

[1] L. Khezami, R. Capart, J. Hazard. Mater. 123 (2005) 223.
[2] J. Gañan, C. González-García, J. González, E. Sabio, A. Macías-García, M. Díaz-Díez, Appl. Surf. Sci. 238 (2004) 347.
[3] M. Sekar, V. Sakthi, S. Rengaraj, J. Colloid Interface Sci. 279 (2004) 307.
[4] S. Babel, T. Kurniawan, Chemosphere 54 (2004) 951.
[5] R. Shawabkeh, D. Rockstraw, R. Bhada, Carbon 40 (2002) 781.
[6] M. Kobya, E. Demirbas, E. Senturk, M. Ince, Bioresour. Technol. 96 (2005) 1518.
[7] C. Durán-Valle, M. Gómez-Corzo, J. Pastor-Villegas, J. Anal. Appl. Pyrolysis 73 (2005) 59.

[8] S. Yenisoy-Karakas, A. Aygun, M. Gunes, E. Tahtasakal, Carbon 42 (2004) 477.
[9] M. Stöcker, Micropor. Mesopor. Mater. 82 (2005) 257.
[10] N. Katada, T. Takeguchi, T. Suzuki, T. Fukushima, K. Inagaki, S. Tokunaga, H. Shimada, K. Sato, Y. Oumi, T. Sano, K. Segaw, K. Nakai, H. Shoji, P. Wu, T. Tatsumi, T. Komatsu, T. Masuda, K. Domen, E. Yoda, J.N. Kond, T. Okuhar, Y. Kageyama, M. Niwa, M. Ogura, M. Matsukata, E. Kikuchi, N. Okazaki, M. Takahashi, A. Tada, S. Tawada, Y. Kubota, Y. Sugi, Y. Higashio, M. Kamada, Y. Kioka, K. Yamamoto, T. Shouji, Y. Arima, Y. Okamoto, H. Matsumoto, Appl. Catal. A General 283 (2005) 63.
[11] R. Shawabkeh, A. Al-Harahsheh, M. Hami, A. Khlaifat, Fuel 83 (2004) 981.
[12] R. Vaughan Jr., B. Reed, Water Res. 39 (2005) 1005.
[13] D. Nguyen-Thanh, T. Bandosz, Carbon 43 (2005) 359.
[14] I. Eswaramoorthi, A. Geetha Bhavani, N. Lingappan, Appl. Catal. A General 253 (2003) 469.
[15] F. Tomás-Alonso, J. Latasa, Fuel Process. Technol. 86 (2004) 191.
[16] Z. Hu, E. Vansant, Carbon 33 (1995) 1293.
[17] J. Gimknez, M. Aguado, S. Cervera-March, J. Mol. Catal. A Chem. 105 (1996) 67.
[18] T. Dantas, A. Neto, M. Moura, Water Res. 35 (2001) 2219.
[19] K. Aoki, C. Wang, Langmuir 17 (2001) 7371.
[20] L. Ballice, M. Yüksel, M. Salam, H. Schulz, Fuel 76 (1997) 375.
[21] M. Tuttle, M. Goldhaber, Talanta 33 (1986) 935.
[22] M. Duman, S. Duman, T. Lyons, M. Avci, E. Izdar, E. Demirkurt, Mar. Geol. 227 (2006) 51.
[23] I. Mochida, S. Kawano, Ind. Eng. Chem. Res. 30 (1991) 2322.
[24] E. Dimotakis, M. Cal, J. Economy, M. Rood, S. Larson, Environ. Sci. Technol. 29 (1995) 1876.
[25] K. Benak, L. Dominguez, J. Economy, C. Mangun, Carbon 40 (2002) 2323.
[26] T. Yang, A. Lua, J. Colloid Interface Sci. 267 (2003) 408.
[27] A. Puziy, O. Poddubnaya, A. Martínez-Alonso, F. Suárez-García, J. Tascón, Carbon 41 (2003) 1181.
[28] J. Guo, A. Lua, Micropor. Mesopor. Mater. 32 (1999) 111.
[29] R. Arriagada, R. Garcia, M. Molina-Sabio, F. Rodriguez-Reinoso, Micropor. Mater. 8 (1997) 123.
[30] H. Chiang, C. Huang, P. Chiang, Chemosphere 47 (2002) 257.
[31] S. Shin, J. Jang, S. Yoon, I. Mochida, Carbon 35 (1997) 1739.
[32] A. El-Hendawy, Carbon 41 (2003) 713.
[33] M. Kosmulski, J. Colloid Interface Sci. 253 (2002) 77.
[34] I. Smiciklas, S. Milonjic, P. Pfendt, S. Raicevic, Sep. Purif. Technol. 18 (2000) 185.
[35] H. Tel, Y. Alta, M. Taner, J. Hazard. Mater. 112 (2004) 225.
[36] P. Rana, N. Mohan, C. Rajagopal, Water Res. 38 (2004) 2811.
[37] P. Soo-Jin, J. Yu-Sin, J. Colloid Interface Sci. 249 (2002) 458.
[38] C. Huang, Y. Hsieh, S. Park, M. Corapciogiu, A. Bower, H. Elliot, in: J. Patterson, R. Passino (Eds.), Metals Speciation, Separation, and Recovery, Lewis Pub., Chelsea, MI, 1987.
[39] D. Aggarwal, M. Goyal, R. Bansal, Carbon 37 (1999) 1989.